Electronic Supplementary Material (ESI) for Chemical Communications.
This journal is © The Royal Society of Chemistry 2019

Water-soluble titanium-polyoxomolybdate with external μ_3 bridging oxygen coordination on lacunary Keggin structure

Ming Xu, Ting Wang, Fengyan Li ,* Wenjuan Xu, Yue Zheng and Lin Xu *

Key Laboratory of Polyoxometalates Science of Ministry of Education, College of Chemistry, Northeast Normal University, Changchun 130024, P. R. China. E-mail: linxu@nenu.edu.cn, lify525@nenu.edu.cn

CONTENTS

Section 1 Collected Examples of Ti-containing POMs

Table S1. Collected Examples of Ti-containing POMs

Ti-containing POMs	Structure	The coordination mode of O in Ti-O band	Water -solubility	Synthetic method	Ref.
$K_6(H_3O)_8[\{PMo_9O_{34}TiO\}_2]•32H_2O$	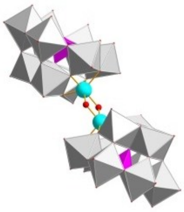	μ_2-O and μ_3-O	water-soluble	conventional aqueous solution sythesis	This work
$(NH_3CH_2CH_2NH_2)_5Na[Ti_2Mo_{12}O_{30}(PO_4)(HPO_4)_4(H_2PO_4)_3]\cdot 6H_2O$	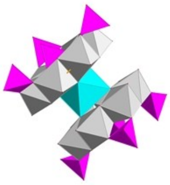	μ_3-O	water-insoluble	hydrothermal sythesis	1
$[C_5H_5NH]_5[(NiOH)_2Mo_{10}O_{36}(PO_4)Ti_2]$	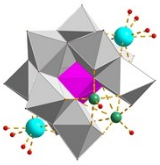	μ_2-O and μ_3-O	water-insoluble	hydrothermal sythesis	2
$[(n-C_4H_9)_4N]_2[HCp^*TiMo_5O_{18}]$	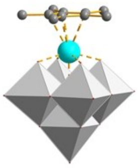	μ_2-O and μ_6-O	water-insoluble	Organic solvent sythesis	3
$(^nBu_4N)_3[(^iPrO)TiMo_5O_{18}]$	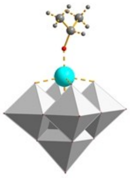	μ_2-O and μ_6-O	water-insoluble	Organic solvent sythesis	4
$(^nBu_4N)_3[(2-CHOC_6H_4O)TiMo_5O_{18}]$	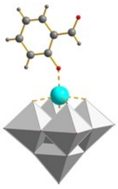	μ_2-O and μ_6-O	water-insoluble	Organic solvent sythesis	5

$(^{n}Bu_4N)_6[(\mu\text{-}O)(TiMo_5O_{18})_2]$	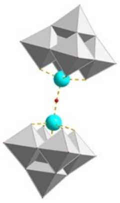	μ_2-O and μ_6-O	water-insoluble	Organic solvent sythesis	5

References

[1] L. Xu, Y. Q. Sun, E. B. Wang, M. Q. Li, C. W. Hu, and R. D. Huang, *Journal of Chemical Crystallography.,* 2000, 721-726.

[2] H. Zhang, Y. G. Li, L. Y. Duan, Y. Lan, E. B. Wang, C. W. Hu, Y. G. Yao, J. T. Chen, and S. Gao, *Journal of Solid State Chemistry.,* 2003, **170**, 232-236.

[3] H. Akashi, J. Chen, H. Hasegawa, M. Hashimoto, T. Hashimoto, T. Sakuraba, A. Yagasaki, *Polyhedron.,* 2003, **22**, 2847-2854.

[4] R. J. Errington, L. Coyle, P. S. Middleton, C. J. Murphy, W. Clegg, R. W. Harrington, *J Cluster Sci.,* 2010, **21**, 503-514.

[5] L. Coyle, P. S. Middleton, C. J. Murphy, W. Clegg, R. W. Harrington and R. J. Errington, *Dalton Trans.,* 2012, **41**, 971–981.

Section 2 Synthesis, Crystal Data, and Structures of 1

2.1 Synthesis

Materials: All chemicals and solvents were commercially purchased and used without further purification.

Synthesis of 1: $H_3[PMo_{12}O_{40}]$ (PMo_{12}) (0.9824g, 0.54 mmol) was dissolved in 15ml 1M KAc/HAc buffer solution (pH=5.28), after the solution was stirred for around 30 min, L-Threonine (0.1204g 1.01 mmol) and $K_7H[Ti_6O_9(ida)_6]Cl_2$ (Ti_6) (0.1536g, 0.08 mmol) were successively added. This solution was stirred for another 2 h, filtered and left to evaporate slowly. Colorless blockshaped crystals were obtained after four days, which were then collected by filtration and air-dried. Yield: 0.38 g, (15%, based on Mo). IR (in cm^{-1}): 3425 (s), 1628 (w), 1574 (w), 1404 (s), 1280 (w), 1064(s), 1001(w), 900 (w), 844 (w), 737 (s) 672 (w), 512 (w). Elemental analysis, calc. for $K_6H_{88}Mo_{18}O_{110}P_2Ti_2$: K 5.91, P 1.56 Mo 43.52 Ti 2.51 %; Found K 5.82 P 1.48 Mo 42.17 Ti 2.38 %.

2.2 Crystal Data

Table S2. Crystal Data and Structure Refinements for 1

	1
Empirical formula	$\mathbf{K_6H_{88}Mo_{18}O_{110}P_2Ti_2}$

Formula weight	**3967.82**
Temperature/K	**273.0**
Crystal system	**triclinic**
Space group	**P-1**
a/Å	**12.3750(4)**
b/Å	**13.5901(5)**
c/Å	**16.7251(7)**
α/°	**103.174(3)**
β/°	**110.846(3)**
γ/°	**94.834(3)**
Volume/Å^3	**2516.86(17)**
Z	**1**
ρ_{calc}g/cm^3	**2.327**
μ/mm^{-1}	**2.690**
F(000)	**1648.0**
Crystal size/mm^3	**0.23 × 0.18 × 0.15**
Radiation	**MoKα (λ = 0.71073)**
2Θ range for data collection/°	**6.976 to 58.746**
Index ranges	**$-16 \leq h \leq 16$, $-16 \leq k \leq 18$, $-22 \leq l \leq 19$**
Reflections collected	**19103**
Independent reflections	**11489 [R_{int} = 0.0310, R_{sigma} = 0.0607]**
Data/restraints/parameters	**11489/0/513**
Goodness-of-fit on F^2	**1.040**
Final R indexes [I>=2σ (I)]	**$R_1{}^a$ = 0.0515, $wR_2{}^b$ = 0.1452**
Final R indexes [all data]	**R_1 = 0.0688, wR_2 = 0.1618**
Largest diff. peak/hole / e Å^{-3}	**2.75/-1.31**

$^aR1 = \Sigma||F_o| - |F_c||/\Sigma|F_o|$. $^bwR2 = \{\Sigma[w(F_o^2 - F_c^2)^2]/\Sigma[w(F_o^2)^2]\}^{1/2}$.

Single-crystal X-ray diffraction: Single-crystal X-ray diffraction data for **1** was recorded on a Bruker Apex CCD II area-detector diffractometer with graphitemonochromated MoKα radiation (λ = 0.71073 Å) at 296(2) K. Absorption corrections were applied using multi-scan technique and performed by using the SADABS program[1] . The structures of 1 was solved by direct methods and refined on F^2 by fullmatrix leastsquares methods by using the SHELXTL package[2]. The numbers of lattice water molecules and counter cations for **1** was estimated by the results of elemental analyses, TG curves, and calculations of electron count in the voids with SQUEEZE[3]. During the refinement, all the non-H atoms were refined anisotropically. In the crystal structure, no H atoms on these O atoms could be found from the difference Fourier map. All H atoms on solvent water molecules were included into the formula directly. The highest residue peak 2.750 eA^3 and the deepest hole is -1.310 eA^3. About 9 solvent water molecules, 6 K^+ cations were found from the Fourier maps, however, there are still a very large accessible solvent voids in the crystal structure calculated by SQUEEZE subroutine of PLATON software, indicating that some more water molecules should exist in the structure, but cannot be found from the weak residual electron peaks. Based on the TGA curve and elemental analyses, another 31 H_2O were included into the molecular formula directly. CCDC 1964911 (**1**) contains the supplementary crystallographic data for this paper.

References

[1] Sheldrick, G. SADABS; ver. 2.10; *University of Gottingen: Göttingen.,* Germany, **2003**.

[2] A. L. Spek, *Acta Cryst.,* **2015** . C71, 9-18.

[3] Spek, A. L. PLATON, *A Multipurpose Crystallographic Tool;* Utrecht University, Utrecht, The Netherlands, **2003**.

2.3 Structures of 1

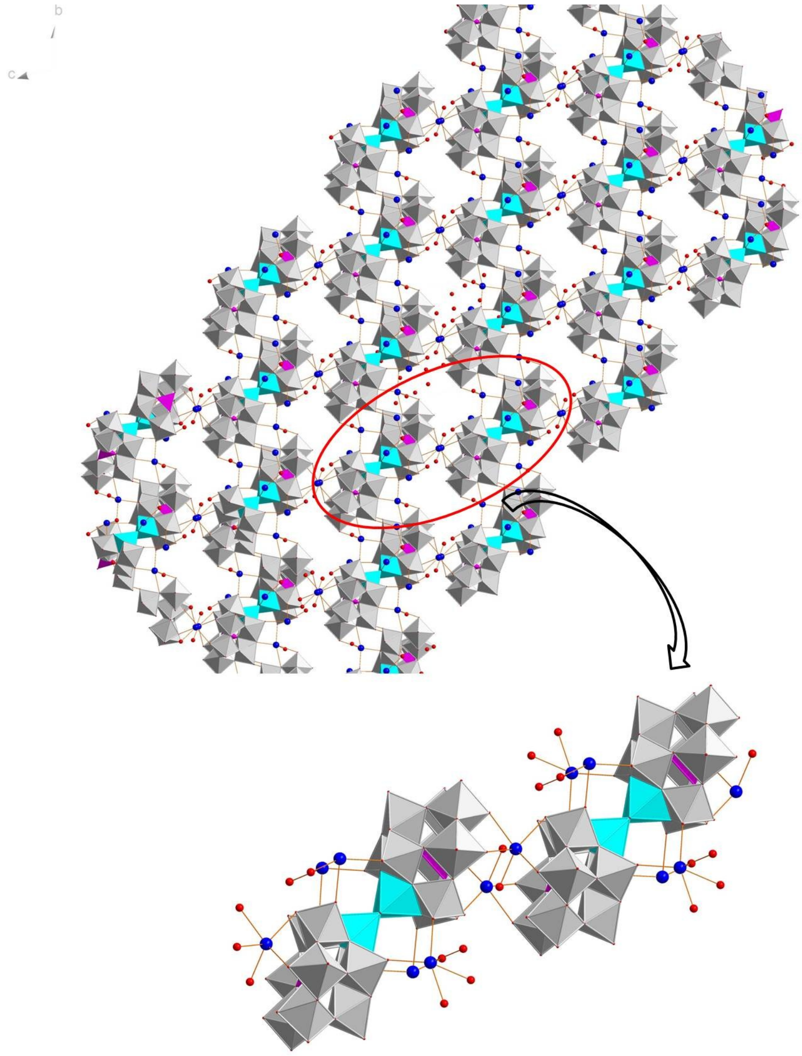

Fig. S1. 3D packing structure of compound 1 along a-axis.

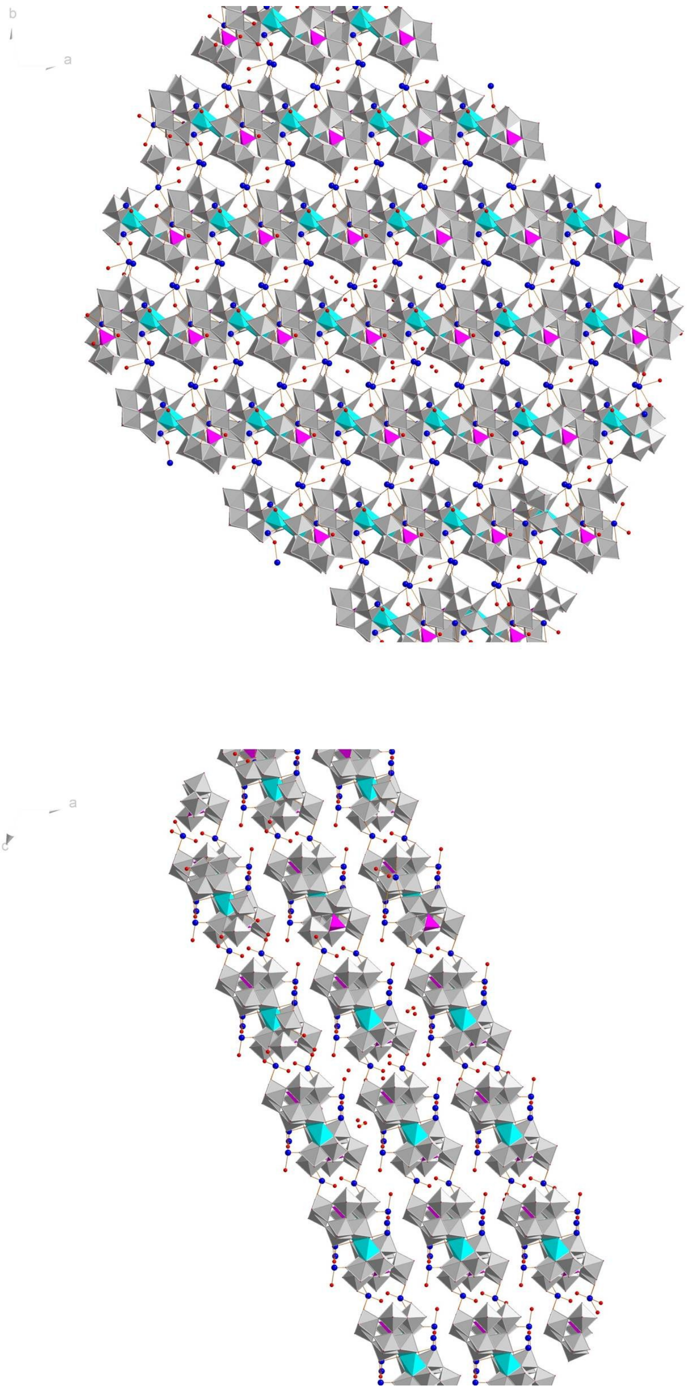

Fig. S2. 3D packing structure of compound **1** along b-axis and c-axis.

2.4 The BVS Calculation Result of All the P Mo and Ti Atoms

Table S3. The BVS Calculation Result of All the P Mo and Ti Atoms

Code	Bond Valence	Code	Bond Valence
P_1	4.922	Ti_1	4.171
Mo_1	6.087	Mo_2	6.082
Mo_3	6.048	Mo_4	6.091
Mo_5	6.105	Mo_6	5.921
Mo_7	6.131	Mo_8	6.173
Mo_9	6.035		

2.5 Selected Bond Lengths and Angles for the Ti Atoms in 1

Table S4. Selected bond lengths [Å] and angles [°] for the Ti atoms in 1

Atom-Atom	Length/Å
Ti_1-O_{20}	2.065(5)
Ti_1-O_{21}	1.923(5)
Ti_1-O_{29}	1.923(5)
Ti_1-O_{30}	1.925(4)
Ti_1-O_{45}	1.936(5)
Atom-Atom-Atom	**Angles/ [°]**
Ti_1-O_{20}-Mo_5	103.1(2)
Ti_1-O_{20}-Mo_6	102.7(2)
Ti_1-O_{21}-Mo_5	105.3(2)
Ti_1-O_{21}-Mo_9	104.8(2)
Ti_1-O_{29}-Mo_7	99.2(2)
Ti_1-O_{29}-Mo_9	98.6(2)
Ti_1-O_{30}-Mo_6	105.1(2)
Ti_1-O_{30}-Mo_7	104.8(2)
O_{21}-Ti_1-O_{20}	77.5(2)
O_{21}-Ti_1-O_{30}	106.4(2)
O_{21}-Ti_1-O_{45}	90.1(2)
O_{29}-Ti_1-O_{20}	144.0(2)
O_{29}-Ti_1-O_{21}	81.4(2)
O_{29}-Ti_1-O_{30}	80.9(2)
O_{30}-Ti_1-O_{20}	77.6(2)
O_{30}-Ti_1-O_{45}	163.1(2)
O_{45}-Ti_1-O_{20}	103.0(3)
O_{45}-Ti_1-O_{45}^3	74.7(2)

Section 3 Experimental Section

3.1 Materials and Physical Measurements

Characterization: Elemental analysis of K, P, Mo, and Ti were performed with a Leaman inductively coupled plasma (ICP) spectrometer; C was performed on a Perkin-Elmer 2400 CHN elemental analyzer. IR spectra were recorded on an Alpha Centauri FTIR spectrophotometer on pressed KBr pellets in the range 400~4000 cm^{-1}. Water contents were determined by TG analyses on a PerkinElmer TGA7 instrument in flowing N_2 with a heating rate of 10 °C min^{-1}.

Electrochemical experiments: Electrochemical measurements were carried out on a CHI 660c electrochemical workstation at room temperature. Compound **1** was dissolved in 0.4 M Na_2SO_4 solution. A conventional three-electrode system was used with a 1.5 mm glassy carbon electrode (GCE) as working electrode, an Ag/AgCl as reference electrode, and a platinum wire counter electrode. The glassy carbon working electrodes were polished with alumina on polishing pads, rinsed with distilled water, and sonicated in H_2O before each experiment.

3.2 UV-Vis spectra

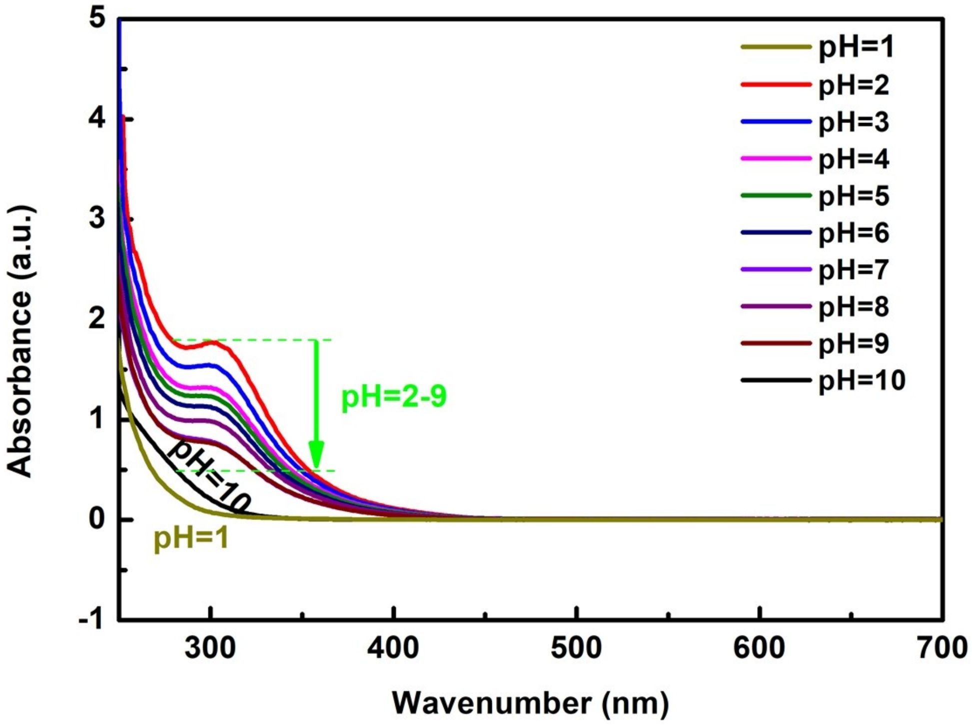

Fig. S3. The UV-vis spectroscopy of aqueous solution stabilities in different pH value of 1.

3.3 Cyclic Voltammetry

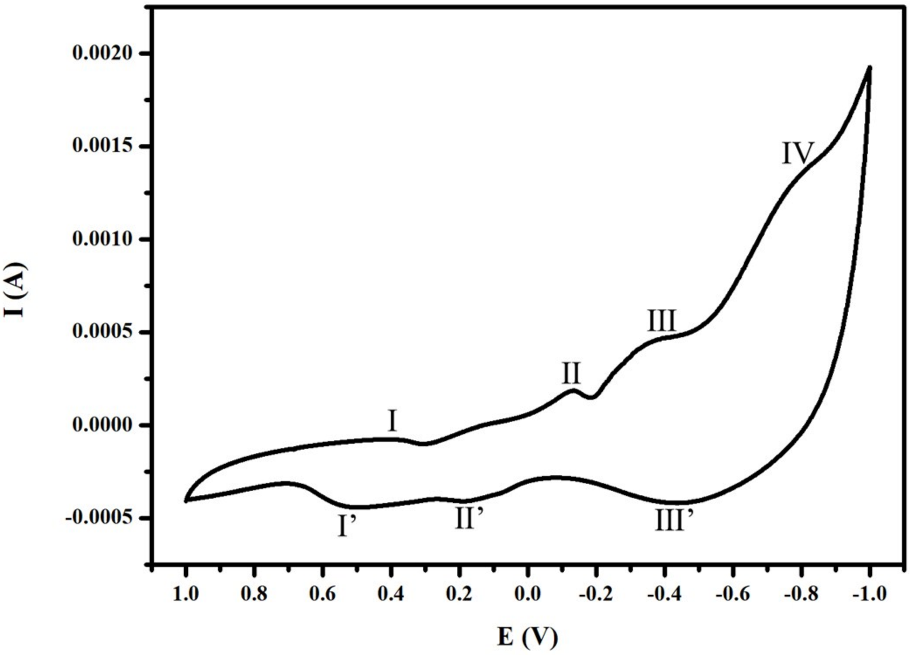

Fig. S4. The cyclic voltammograms of the compound 1 in 0.4M Na_2SO_4 solution at 500 mVs^{-1}. The half-wave potentials $E_{1/2} = (E_{pc} + E_{pa})/2$ are +0.51 V, +0.04 V and −0.41 V, respectively, at a scan rate of 500 mVs^{-1}. Redox peaks I-I’, II-II’ and III-III’ correspond to the reduction and oxidation through two-, four- and six- electron processes of Mo^{VI}, respectively.[1,2] Compared with the CV of titanium-free trilacunary cluster PMo_9, the additional reduction peak at -0.84 V should be attributed to the reduction of Ti center.[3,4]

References

[1] W. B. Song, X. Chen, Y. X. Jiang, Y. Liu, C. Q. Sun, X. H. Wang, *Anal. Chem. Acta.,* 1999, 394, 73-80.

[2] S. Q. Liu, Z. Y. Tang, A. L. Bo, E. K. Wang, S. J. Dong, *J. Electroanal. Chem.,* 1998, 458, 87-97.

[3] K. Y. Wang, Z. G. Lin, B. S. Bassil, X. L. Xing, A. Haider, B. Keita, G. J. Zhang, C. Silvestru, and U. Kortz, *Inorg. Chem.,* 2015, 54, 10530-10532.

[4] F. Hussain, B. S. Bassil, U. Kortz, O. A. Kholdeeva, M. N. Timofeeva, P. D. Oliveira, B. Keita, and L. Nadjo, *Chem. Eur. J.,* 2007, 13, 4733-4742.

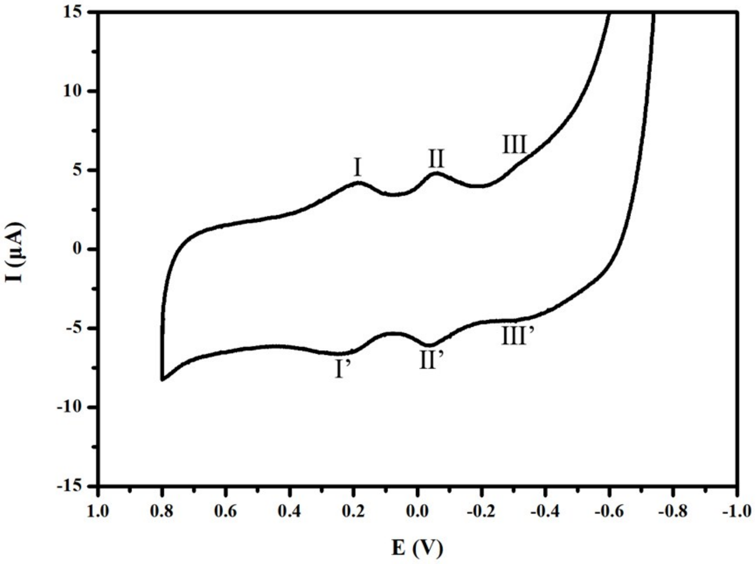

Fig. S5. The cyclic voltammograms of the $(TBA)_nPMo_9O_{34}$ in 1M $LiClO_4$ acetonitrile solution at 500 mVs^{-1}.

3.4 Benzaldehyde Oxide Experimental Section

General procedure for the oxidation of benzaldehyde: PMo_9Ti (6.0 mg, 0.109 mol %), benzaldehyde (159.0mg 1.5mmol), H_2O_2 (3ml), and H_2O (5ml) were added to a glass bottles. Under the simulated sunlight, the mixture was stirred at 60 ℃, and the yields were calculated from gas chromatography. The ability of the PMo_9Ti POM catalyst to be recycled was also evaluated. After the reaction, benzaldehyde and benzoic acid in the system were extracted with ethyl acetate. Then the photocatalyst powder was obtained by evaporating the solution. In the following step, fresh H_2O_2 (3ml), H_2O (5ml) and benzaldehyde (159mg, 1.5mmol) were mixed with the dried photocatalyst powder for the cycling experiments.

Table S5 The study of experimental mechanism [a]

Entry	Additive 1	Additive 2	Light	Cat./Mol%	T/°C	Yield %^{a}
1	H_2O_2	isopropanol	AM 1.5G	0	60	28.7
2	H_2O_2	isopropanol	AM 1.5G	0.109	60	37.8
3	H_2O_2	Ammonium oxalate	AM 1.5G	0.109	60	46.5
4	H_2O_2	1,4-benzoquinone	AM 1.5G	0.109	60	63.3

[a] Reaction Condition: PMo_9Ti (0.109 mol%), benzaldehyde (1.5mmol), H_2O_2 (3mL), H_2O (5mL), 60°C.

Table S6 Recycling experiments of catalyst.[a]

Run Time	**1**	**2**	**3**
Yield [%]	**79.1**	**73.1**	**72.7**

[a] Reaction Condition: PMo$_9$Ti(0.109 mol%), benzaldehyde (1.5mmol), H_2O_2 (3mL), H_2O (5mL), 60°C.

Section 4 Supplementary Physical Characterizations

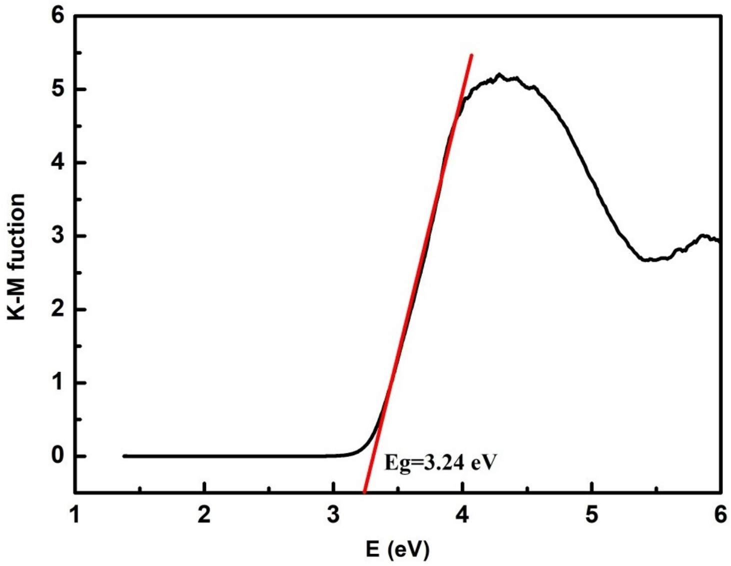

Fig. S6. The diffuse reflectance UV-vis-NIR spectra of K-M function *vs.* energy (eV) of **1.**

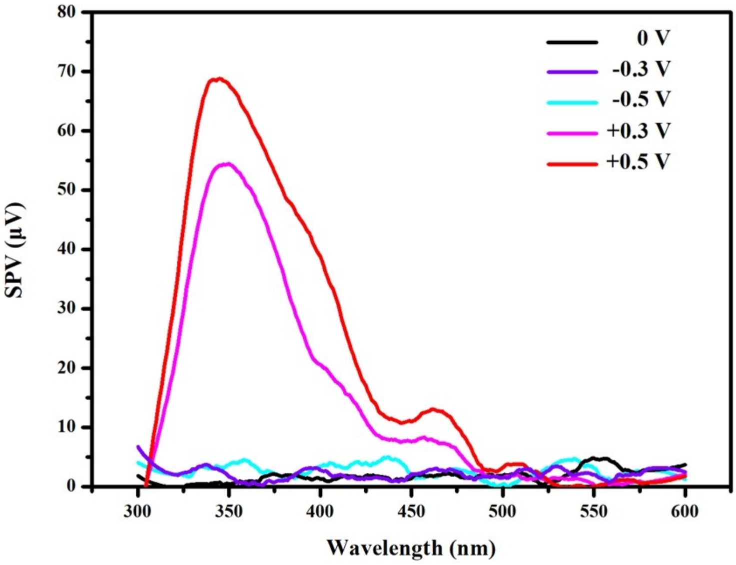

Fig. S7. The surface photovoltage spectra (SPS) and electric field-induced surface photovoltage spectra (EFISPS) under different positive and negative electric fields of compound 1.

Fig. S7 shows the the SPS and EFISPS of **1** in the range of 300-600 nm when the external electric fields are -0.3, -0.5, 0, +0.3, and +0.5 V, respectively. No obvious surface photovoltage (SPV) response was observed with zero or negative electric field. When a positive electric field is employed, compound **1** displays the pronounced SPV response bands in the range of 300-500 nm assigned to the exciton transition. The SPV response intensities of the compound rapidly rise with the positive fields increasing due to the same direction of added-outer as built-in field, which suggest that compound **1** possesses the characteristic of n-type semiconductor.[1,2]

References

[1] G. F. Hou, L. H. Bi, B. Li, and L. X. Wu, *Inorg. Chem.,* 2010, **49**, 6474-6483.

[2] S. Z. Li, J. W. Zhao, P. T. Ma, J. Du, J. Y. Niu, and J. P. Wang, *Inorg. Chem.,* 2009, **48**, 9819-9830.

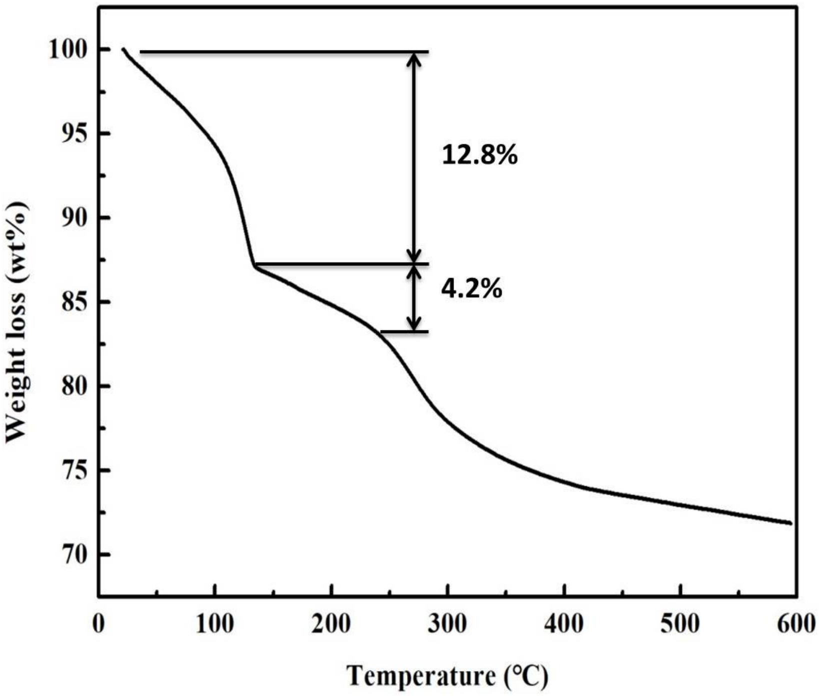

Fig. S8. TGA curve of compound 1.

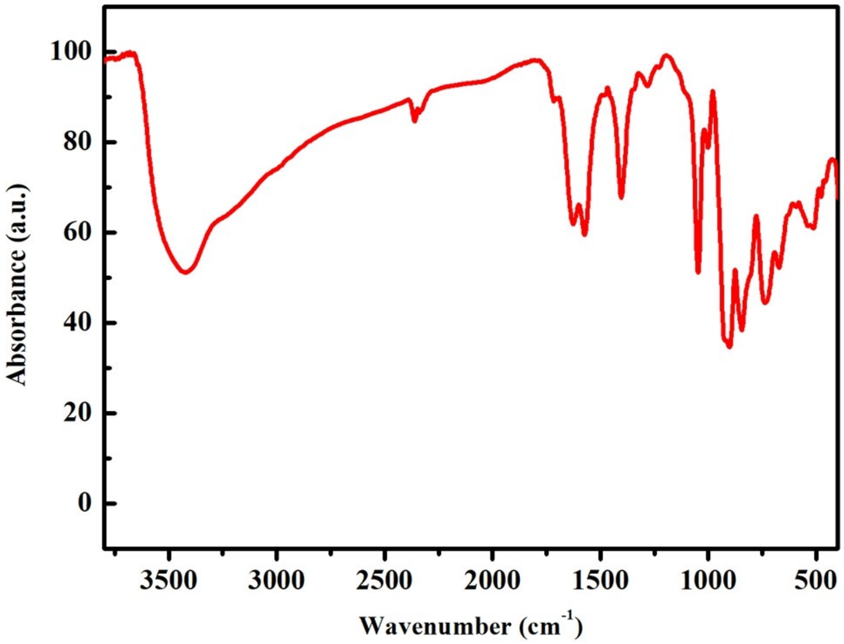

Fig.S9. IR spectra of compound **1**.

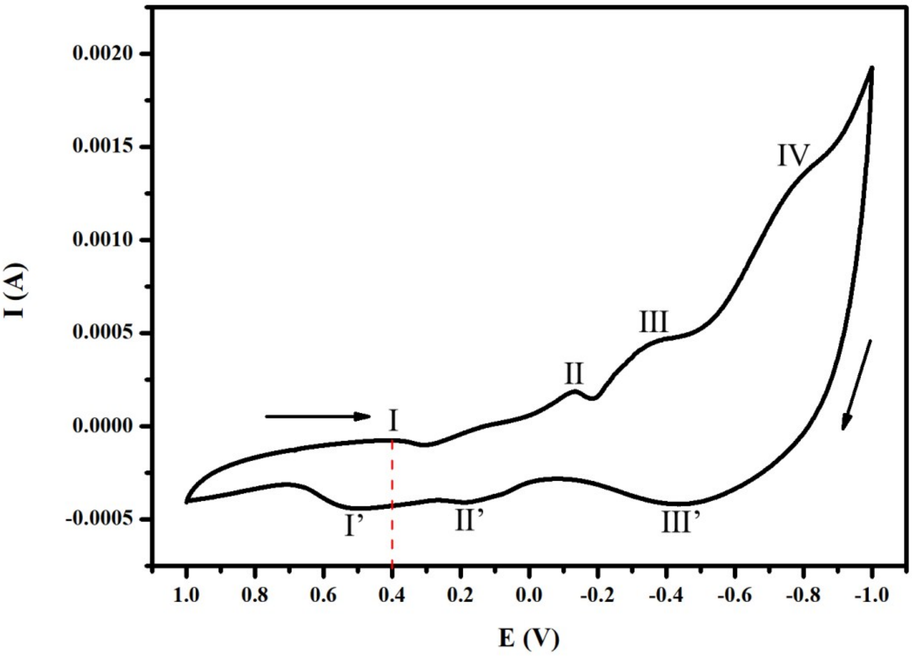

Fig. S10. The cyclic voltammogram (CV) of compound **1**, in which the LUMO level is estimated from the first reduction potential in the CV curves to be 0.4 V vs. Ag/AgCl, being equal to 0.597 V vs. NHE and -5.097 eV vs. vacuum (ref. *ACS Appl. Mater. Interfaces.,* 2015, **7**, 13714−13721.). The HOMO level of compound **1** can be derived to be -8.337 eV from the equation of E (LUMO) = E (HOMO) + E_g.